JACS
JOURNAL OF THE AMERICAN CHEMICAL SOCIETY

ARTICLE

pubs.acs.org/JACS

An Advanced Lithium Ion Battery Based on High Performance Electrode Materials

Jusef Hassoun,[†] Ki-Soo Lee,[‡] Yang-Kook Sun,[*,‡] and Bruno Scrosati[*,†,‡]

[†]Department of Chemistry, University of Rome Sapienza, 00185, Rome, Italy

[‡]WCU, Department of Energy Engineering, Hanyang University, Seoul 133-792, South Korea

ABSTRACT: In this paper we report the study of a high capacity Sn−C nanostructured anode and of a high rate, high voltage $Li[Ni_{0.45}Co_{0.1}Mn_{1.45}]O_4$ spinel cathode. We have combined these anode and cathode materials in an advanced lithium ion battery that, by exploiting this new chemistry, offers excellent performances in terms of cycling life, i.e., ca. 100 high rate cycles, of rate capability, operating at 5C and still keeping more than 85% of the initial capacity, and of energy density, expected to be of the order of 170 Wh kg^{-1}. These unique features make the battery a very promising energy storage for powering low or zero emission HEV or EV vehicles.

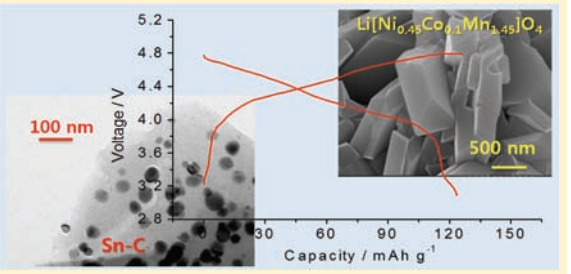

1. INTRODUCTION

The automobile market is presently aimed toward the development of low emission cars, such as hybrid electric vehicles (HEVs) and plug-in hybrid electric vehicles (PHEVs), and of zero emission, full electric vehicles (EVs). Making these sustainable vehicles a reality still depends on the availability of suitable energy storage systems such as, ideally, high energy lithium ion batteries. Indeed, these batteries have achieved a leading role in the consumer electronics market where they are the power sources of choice of a series of very popular portable devices.[1] Further improvements in terms of energy and power density, however, are still required for making these systems suitable for application in the electric vehicle sector. Enhancements in energy density necessarily require the passage from the present lithium ion technology to novel, advanced chemistries based on high performance electrode materials. Good examples are lithium metal alloy anodes[2−5] and spinel cathodes.[6−9] It is expected that advancements in lithium ion battery technology can be achieved by combining these high performance electrode materials in a complete cell configuration.

In a previous paper we described a novel design battery formed by combining a high capacity nanostructured tin−carbon (Sn−C) anode with a high voltage $LiNi_{0.5}Mn_{1.5}O_4$ spinel cathode.[10] The excellent performance in terms of cycle life and rate capability confirmed the validity of the concept, thus encouraging us to extend the approach for obtaining other, advanced lithium ion battery chemistries. In this work we disclose an important example based on a Sn−C anode having an optimized morphology with a high rate, new $Li[Ni_{0.45}Co_{0.1}Mn_{1.45}]O_4$ cathode.

2. EXPERIMENTAL SECTION

$Li[Ni_{0.45}Co_{0.1}Mn_{1.45}]O_4$ was prepared by a coprecipitation method, similar to that described in previous papers.[11] Stochiometric proportions of high purity $NiSO_4 \cdot 6H_2O$ (Kanto Co, Japan), $CoSO_4 \cdot 7H_2O$ (Kanto Co, Japan), and $MnSO_4 \cdot 5H2O$ (Kanto Co, Japan) were used as the starting materials for the synthesis of $[Ni_{0.225}Co_{0.05}Mn_{0.725}](OH)_2$. An aqueous solution of $NiSO_4 \cdot 6H_2O$, $CoSO_4 \cdot 7H_2O$, and $MnSO_4 \cdot 5H_2O$ with a concentration of 2.4 mol L^{-1} was pumped into a continuously stirred tank reactor (CSTR, 4 L) under a N_2 atmosphere. Simultaneously, a NaOH solution (aq) of 4.8 mol L^{-1} and the desired amount of NH_4OH solution (aq. chelating agent) were also separately pumped into the reactor. The concentration of the solution, pH, temperature, and stirring speed of the mixture in the reactor were carefully controlled. The precursor powders were then obtained through filtering, washing, and drying in a vacuum oven overnight. $Li[Ni_{0.45}Co_{0.1}Mn_{1.45}]O_4$ was prepared by mixing LiOH and $[Ni_{0.225}Co_{0.05}Mn_{0.725}](OH)_2$ with a molar ratio of 1:2, followed by heat treatment at 850 °C for 20 h in air atmosphere. The Sn−C synthesis followed the route described in previous papers.[12]

Prior to full lithium ion cell assembly, the Sn−C electrode was prelithiated by a surface treatment. This was performed by placing the electrode in direct contact with a Li foil wet by the electrolyte solution for 180 min.[13] The Sn−C pretreatment effect, as well as its rate capability, was studied by galvanostatic cycling with a Maccor series 4000 battery tester of cells formed by coupling the pristine and the pretreated electrode, respectively, with a lithium foil counter electrode in a swagelok T cell using a standard LP30 (EC:DMC 1:1, $LiPF_6$ 1 M, Merck) electrolyte soaked in a Whatman separator.

The $Li[Ni_{0.45}Co_{0.1}Mn_{1.45}]O_4$ and the Sn−C electrodes were prepared by blending the active materials, Super P carbon and polyvinylidene fluoride, in *N*-methyl-2-pyrrolidone. The slurry was then cast on aluminum and copper foil, respectively, and dried overnight under vacuum. The active material loading was of the order of 2 mg cm^{-2} for the Sn−C and of the order of 5 mg cm^{-2} for the $Li[Ni_{0.45}Co_{0.1}Mn_{1.45}]O_4$ electrode. While sufficient for the characterization

Received: November 23, 2010
Published: February 03, 2011

dx.doi.org/10.1021/ja110522x | *J. Am. Chem. Soc.* 2011, 133, 3139–3143

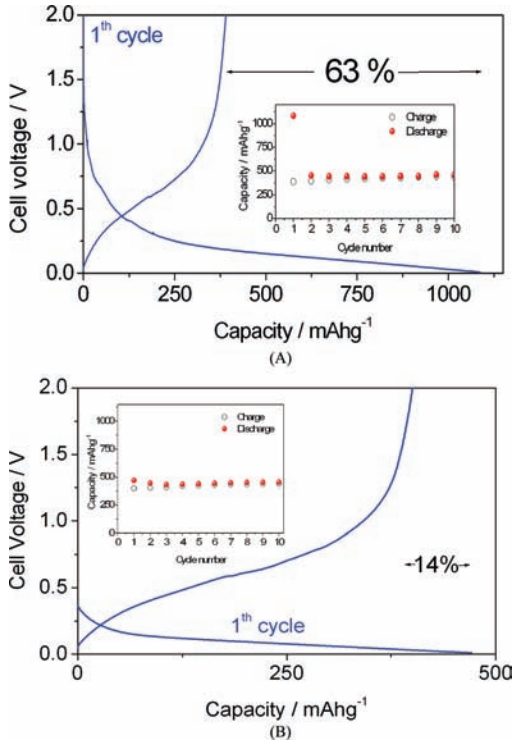

Figure 1. Voltage profiles of a pristine (A) and of a surface-treated (B) Sn−C electrode in a lithium cell. The inset shows the differences in cycle behavior of the two electrodes. Cycling current 80 mA g^{-1}, voltage limits 0.01−2 V. For the treatment procedure, see Experimental Section.

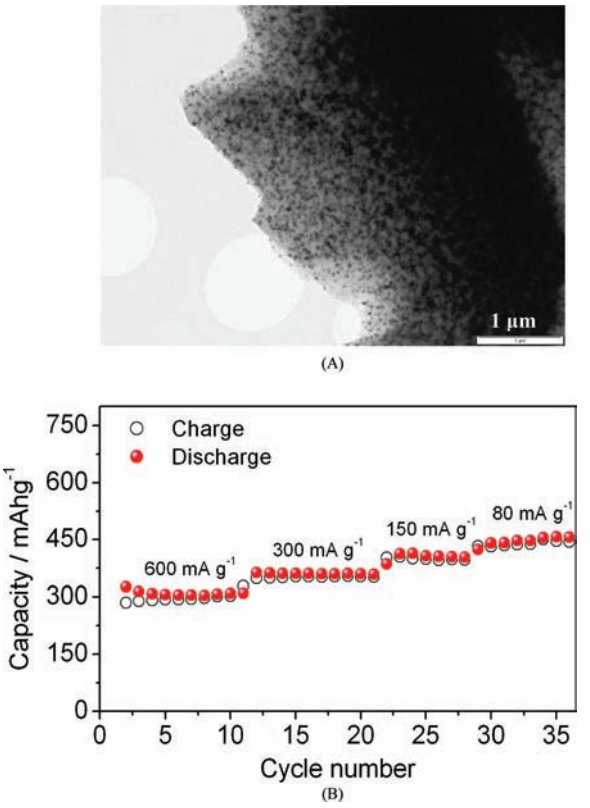

Figure 2. High resolution transmission electron microscopy (HRTEM) images (A) and galvanostatic cycling test in a lithium cell at various currents (B) of the optimized Sn−C nanocomposite anode.

of coin-type laboratory cells, the electrode loading should certainly be increased in case of practical development of the battery.

The potentiodynamic cycling with galvanostatic acceleration (PCGA) test was performed using a VMP Biologic-Science Instrument with stepwise potential scans of 5 mV and a minimum current limit of 10 μA within a 3.5−4.9 V vs Li potential limits. The test was run in a three-electrode cell where the working electrode sample was combined with a lithium foil used as reference and counter electrode. The electrolyte was a 1.2 M $LiPF_6$ solution in ethylene carbonate−ethyl methyl carbonate (3:7 in volume, PANAX ETEC Co., ltd.) soaked in a polyethylene separator (Celgard 2400).

The galvanostatic cycling tests were carried out with a Hosen instrument using 2032 coin-type cells prepared by coupling the electrode under test with a lithium foil counter electrode. A SnC/Li-$[Ni_{0.45}Co_{0.1}Mn_{1.45}]O_4$ battery was evaluated by galvanostatic cycling in a 2032 coin-type cells formed by coupling a pretreated Sn−C anode with a $Li[Ni_{0.45}Co_{0.1}Mn_{1.45}]O_4$ cathode at various C-rates. The battery was cathode limited, and 1C rate referring to the cathode weight was 132 mAh g^{-1}.

The X-ray diffraction was carried out using a Rigaku instrument with Cu−Kα source while the electron microscopy was performed using a JSM 6400 instrument.

3. RESULTS AND DISCUSSION

3.1. The Anode. Lithium metal, Li−M, alloys (M = Sn, Si, Sb, etc.) are very appealing, advanced anode materials, due to their specific capacity that is much higher than that of commercially used graphite.[2−4] However, the use of Li−M alloys has been so far prevented by the large volume expansion−contraction experienced during their electrochemical process in lithium cells. We have shown that the volume stress issue can be efficiently solved by developing suitable electrode morphologies, such as M−C nanocomposites.[12] Indeed, we demonstrated that a Sn−C composite may operate in lithium cells with several hundred cycles, without capacity decay and with discharge (lithium-alloying)−charge (lithium dealloying) efficiency approaching 100%. As reported in a previous paper,[10] the Sn/C weight ratio in this composite is about 45/55 corresponding to a capacity ratio, in terms of mAh g^{-1}, of about 450/50.

Because of its unique properties we have selected this Sn−C composite as the preferred anode material for this work. The anode is basically similar to that previously reported,[12] however, considerably upgraded in terms of surface morphology and rate capability. In particular, the issue of large irreversible capacity that affected our original material has here been successfully addressed by a suitable surface treatment;[13] see also Experimental Section.

Figure 1, which compares the voltage profiles of the first charge−discharge cycle of a lithium cell using a pristine Sn−C electrode (A) and a treated Sn−C electrode (B), demonstrates the beneficial effect of the treatment. A considerably large irreversible capacity (due to the occurrence of side reactions involving electrolyte oxidation with formation of a solid electrolyte interface, SEI) amounting to 63% is shown in the first cycle, after which the electrode assumes the expected steady-state behavior, namely a stable reversible capacity of the order of 500 mAh g^{-1} associated with the electrochemical process involving the alloying of lithium in tin:

$$Sn{-}C + 4.4Li \underset{\text{dealloying}}{\overset{\text{alloying}}{\rightleftharpoons}} Li_{4.4}Sn{-}C \qquad (1)$$

Following the surface treatment, the electrode maintains its high capacity response, however, with a remarkable reduction of

dx.doi.org/10.1021/ja110522x | J. Am. Chem. Soc. 2011, 133, 3139–3143

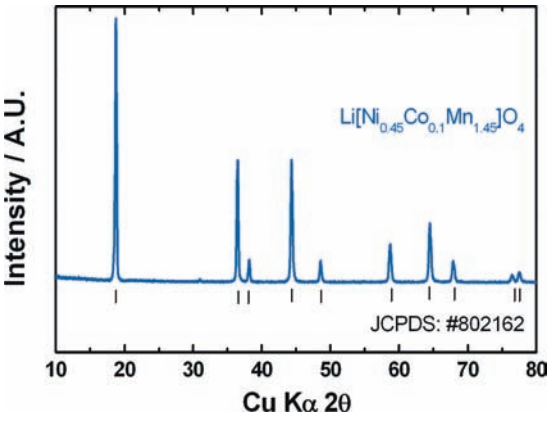

Figure 3. X-ray diffraction patterns of the $Li[Ni_{0.45}Co_{0.1}Mn_{1.45}]O_4$ spinel electrode.

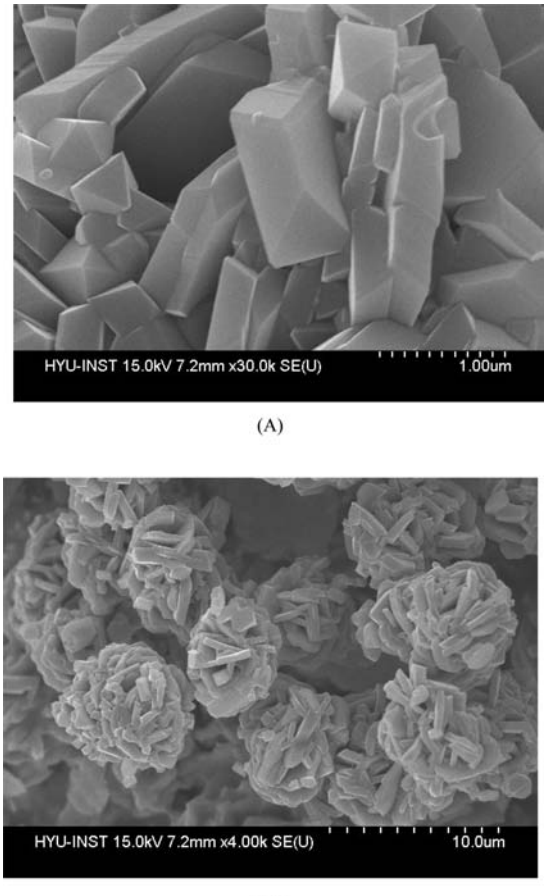

Figure 4. Field emission scanning electron microscopy (FESEM) images of the $Li[Ni_{0.45}Co_{0.1}Mn_{1.45}]O_4$ spinel electrode.

the irreversible capacity, that passed from ca. 680 mAh g^{-1} (63% of irreversibility) to ca. 65 mAh g^{-1}(14% of irreversibility); see Figure 1B.

The Sn−C electrode has been also upgraded in terms of rate capability. Improvement in the morphology, i.e., assuring a uniform distribution of the nanometric tin particles in the amorphous carbon matrix and avoiding any aggregation, allowed the electrode to operate under high current rates. The high resolution transmission electron microscopy (HRTEM) image

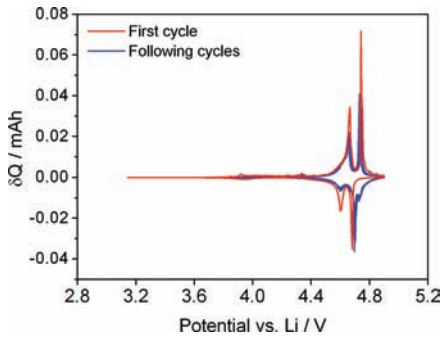

Figure 5. Potentiodynamic cycling with galvanostatic acceleration (PCGA) response of the $Li[Ni_{0.45}Co_{0.1}Mn_{1.45}]O_4$ electrode in a lithium cell. Stepwise potential scans 5 mV, minimum current limit of 10 μA, potential limits 3.5−4.9 V vs Li. Electrolyte EC:EMC 3:7, $LiPF_6$ 1.2 M.

of the upgraded Sn−C electrode in Figure 2A clearly shows that the tin nanoparticles are uniformly dispersed in the carbon matrix. Figure 2B shows the typical response of the Sn−C electrode in a lithium cell, demonstrating that this electrode can indeed operate under a high rate and still keep a high percentage of the maximum capacity, i.e. 300 mAh g^{-1}, at a current of 600 mA g^{-1} (1.2C rate).

3.2. The Cathode. For the progress of lithium ion battery technology, it is highly desirable to replace the common, high cost lithium cobalt oxide with cathodes based on more abundant and more environmentally friendly materials. Good choices are lithium manganese spinels. However, the response of these alternative cathodes in lithium cells is strongly influenced by the particle size and by the presence of doping metals.[14,15] Reduction in the particle size, on one hand, significantly improves the kinetics of the electrochemical lithium insertion/extraction reactions, but on the other hand, increases reactivity for the electrolyte decomposition.[14]

In this work we have addressed this contradictory issue by doping $LiMn_2O_4$ spinel with Ni and Co and, at the same time, by preparing the resulting $Li[Ni_{0.45}Co_{0.1}Mn_{1.45}]O_4$ cathode with particles at micrometric size (in order to avoid electrolyte decomposition) and using a metal ratio that is expected to provide high working voltage and high rate capability. Figure 3 shows the XRD patterns of our $Li[Ni_{0.45}Co_{0.1}Mn_{1.45}]O_4$ material. The pattern confirms the well-crystallized cubic spinel structure with *Fd*3*m* space group (JCPDS: #802162).

Figure 4 shows the field emission scanning electron microscopy (FESEM) images of the optimized $Li[Ni_{0.45}Co_{0.1}Mn_{1.45}]O_4$ material. Image A clearly reveals that the particle size is effectively of the micrometer order, and image B that these particles are organized in aggregates with a highly uniform distribution and shape. This particular morphology is assumed to be the most favorable in terms of electrode performance because it assures that a high tap density is maintained at a macroscopic level, and a low particle size at a microscopic level, as indeed demonstrated by the electrochemical tests, see below.

The electrochemical response of the $Li[Ni_{0.45}Co_{0.1}Mn_{1.45}]O_4$ electrode in a lithium cell was first investigated by potentiodinamic cycling with galvanostatic acceleration (PCGA), i.e., a very powerful quasiequilibrium technique that provides useful, quasithermodynamic information on the characteristics of the electrochemical process.[16−18]

Figure 5 shows the PCGA response of the $Li[Ni_{0.45}Co_{0.1}Mn_{1.45}]O_4$ electrode in terms of potential versus step capacity

dx.doi.org/10.1021/ja110522x |*J. Am. Chem. Soc.* 2011, 133, 3139–3143

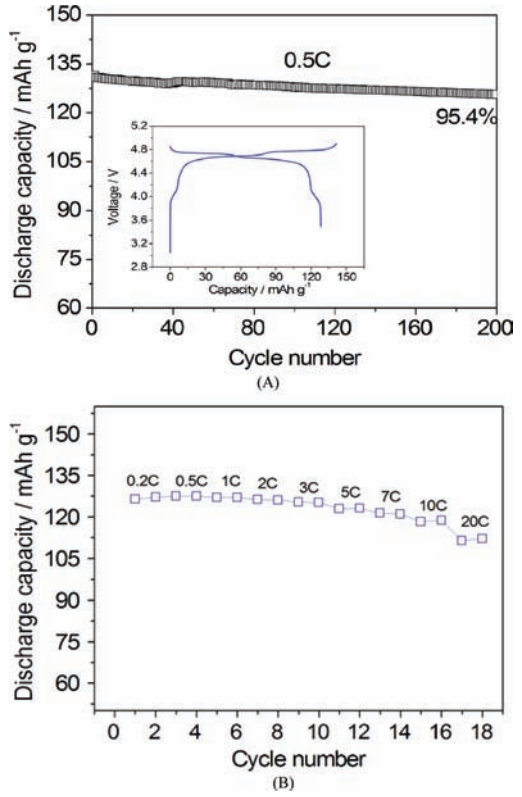

Figure 6. Cycling performance of the galvanostatic test run at 0.5C-rate (A) and at various C-rates (B) of a $Li[Ni_{0.45}Co_{0.1}Mn_{1.45}]O_4$ electrode in a lithium cell (1C = 132 mAh g^{-1}). The inset shows the voltage vs specific capacity profiles of the first charge−discharge cycle. Electrolyte EC:EMC 3:7, $LiPF_6$ 1.2 M.

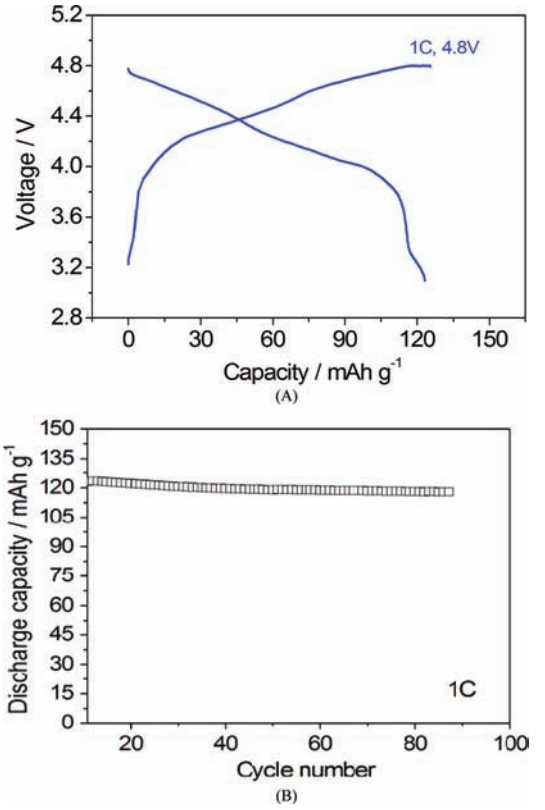

Figure 7. Typical charge−discharge cycle (A) and cycling response of $SnC/Li[Ni_{0.45}Co_{0.1}Mn_{1.45}]O_4$ battery. Voltage limits: 3.1−4.8 V, 1C = 132 mAh g^{-1}. Electrolyte EC:EMC 3:7, $LiPF_6$ 1.2 M.

δQ. The voltage profile of the electrochemical process of our substituted manganese cathode:

$$Li[Ni_{0.45}Co_{0.1}Mn_{1.45}]O_4 \underset{\text{discharge}}{\overset{\text{charge}}{\rightleftharpoons}} xLi + Li(1-x)[Ni_{0.45}Co_{0.1}Mn_{1.45}]O_4 \quad (2)$$

namely the lithium removal (charge)−lithium uptake (discharge) into the spinel structure involves typically one lithium equivalent per mole with an associated theoretical capacity of 132 mAh g^{-1}. Figure 5 shows that the charge process evolves with two high voltage oxidation peaks, at 4.66 V and 4.74 V vs Li, respectively. The process is reversed in discharge in two reduction peaks at a potential value of 4.69 V and 4.61 V vs Li, respectively. These peaks are most likely associated with the Ni^{4+}/Ni^{3+} and Ni^{3+}/Ni^{2+} redox couples.[14] In addition, Figure 5 reveals differences in profile and in the involved capacity when passing from the first cycle to the following one where the response overlaps with excellent reversibility. It is assumed that this initial irreversibility is due to a series of side reactions involving electrolyte oxidation with solid electrolyte interface (SEI) formation, as well as initial reorganization of the spinel structure.[14,19]

Figure 6A shows the cycling response of the $Li[Ni_{0.45}Co_{0.1}Mn_{1.45}]O_4$ electrode in a lithium cell, while the inset illustrates the voltage profile of the first charge−discharge cycle. The working voltage, around 4.7−4.8 V, reflects the expected electrochemical process, see eq 2. The specific capacity of the first charge (150 $mAhg^{-1}$) is higher than the theoretical value (132 mAh g^{-1}) due to the above-discussed initial irreversible process. Under steady-state conditions, the electrode assumes a capacity of 130 mAh g^{-1} and keeps 95.4% of this value for a life extending to 200 cycles. This excellent cycle life and the high operation voltage confirm the validity of our approach in terms of choice of the appropriate morphology and type and condition of doping metals.

Figure 6B shows the electrode response at various C-rate currents. The figure shows the excellent rate-capability of the electrode that can operate at a rate as high as 10C, still keeping 94% of the initial capacity. Again, this result supports the rationality of our approach.

3.3. Full $SnC/Li[Ni_{0.45}Co_{0.1}Mn_{1.45}]O_4$ Battery. After activation,[10,13] the Sn−C anode was combined with the $Li[Ni_{0.45}Co_{0.1}Mn_{1.45}]O_4$ cathode to form a complete lithium ion battery using an ethylene carbonate:ethyl methyl carbonate, EC:EMC, lithium hexafluorophosphate, $LiPF_6$, electrolyte. The battery was tested by galvanostatic cycle runs at various current rates. Figure7A shows a typical charge−discharge cycle at 1C rate, reflecting the process:

$$Sn{-}C + Li[Ni_{0.45}Co_{0.1}Mn_{1.45}]O_4 \underset{\text{discharge}}{\overset{\text{charge}}{\rightleftharpoons}} LixSn{-}C + Li(1-x)[Ni_{0.45}Co_{0.1}Mn_{1.45}]O_4 \quad (3)$$

Figure 7B shows the cycling response of the battery. The tests show that the practical working voltage of the battery ranges between 3.9 V and 4.7 V while the specific capacity, related to the cathode mass, is of the order of 125 mAh g^{-1}. In addition, the battery can cycle at 1C with a very stable capacity delivery.

dx.doi.org/10.1021/ja110522x |J. Am. Chem. Soc. 2011, 133, 3139–3143

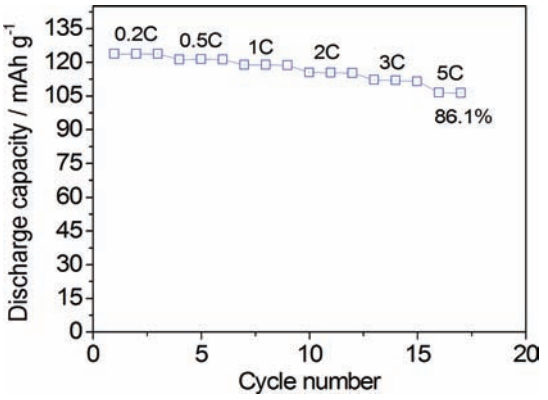

Figure 8. Cycling response at various rates of the SnC/Li-$[Ni_{0.45}Co_{0.1}Mn_{1.45}]O_4$ battery, 1C = 132 mAh g^{-1}. Electrolyte EC: EMC 3:7, $LiPF_6$ 1.2 M.

Taking an average voltage of 4.2 V (see Figure 7A), a top specific energy density value of 500 Wh kg^{-1} is obtained. Assuming a 1/3 reduction factor associated with the weight of the electrolyte, current collector, and aluminum case in a pouch configuration, we obtain a 170 Wh kg^{-1} value that still exceeds that offered by conventional lithium ion batteries chemistry.

Figure 8 shows the response in terms of charge−discharge rates. The battery has high rate capability and can be cycled at 5C, still delivering 110 mAh g^{-1} with only 14% of capacity decay.

Note that the particular electrode morphology adopted here assures not only a battery with stable cycle life and high rate capacity but, due to the high tap density of both electrodes, also an expected high volumetric energy density.

4. CONCLUSION

We believe that the results reported in this work are quite convincing in demonstrating that the battery disclosed here fulfills the requirement expected by advanced energy storage systems. By exploiting a new chemistry based on a combination of a stable, high performance Sn−C anode with a morphologically and structurally optimized $Li[Ni_{0.45}Co_{0.1}Mn_{1.45}]O_4$ cathode, a novel type of lithium ion battery, having high energy content and excellent rate capability, is obtained. To our knowledge, a lithium ion battery having this unique electrode combination has so far never been reported. On the basis of the performance demonstrated here, this battery is a top candidate for powering sustainable vehicles.

AUTHOR INFORMATION

Corresponding Author

yksun@hanyang.ac.kr; bruno.scrosati@uniroma1.it

ACKNOWLEDGMENT

This work was carried out within the WCU (World Class University) program through the Korea Science and Engineering Foundation by Education, Science, and Technology (R31-2008-000-10092). One of us (J.H.) is grateful to the WCU program for a two month fellowship from Hanyang University.

REFERENCES

(1) van SchalkwiJk, W. A.; Scrosati, B., Eds. *Advances in Lithium-ion Batteries*; Kluwer Academic/Plenum Publishers: New York, 2002.

(2) Wachtler, M.; Winter, M.; Besenhard, J. O. *J. Power Sources* **2002**, *105*, 151.

(3) Benedek, R.; Thackeray, M. M. *J. Power Sources* **2002**, *110*, 406.

(4) Chen, Z.; Chevrier, V.; Christensen, L.; Dahn, J. R. *Electrochem. Solid-State Lett.* **2004**, *7*, A310.

(5) Hassoun, J.; Panero, S.; Simon, P.; Taberna, P.-L.; Scrosati, B. *Adv. Mater.* **2007**, *19*, 1632.

(6) Sigala, C; Guyomard, D; Verbaere, A; Piffard, Y; Tournoux, M. *Solid State Ionics* **1995**, *81*, 167.

(7) Kawai, H; Nagata, M.; Tabuchi, M; Tsukamoto, H.; West, A. R. *Chem. Mater.* **1998**, *10*, 3266.

(8) Shigemura, H.; Sakaebe, H; Kageyama, H; Kobayashi, H; West, A. R.; Kanno, R; Morimoto, S; Nasu, S; Tabuchi, M. *J. Electrochem. Soc.* **2001**, *148*, A730.

(9) Ein-Eli, Y.; Howard, W. F.; Lu, S. H.; Mukerjee, S.; MaBreen, J.; Vaughey, J. T.; Thackeray, M. M. *J. Electrochem. Soc.* **1998**, *145*, 1238.

(10) Hassoun, J.; Reale, P.; Panero, S.; Scrosati, B. *Adv. Mater.* **2009**, *21*, 4807.

(11) Oh, S.-W.; Myung, S.-T.; Kang, H.-B.; Sun, Y.-K. *J. Power Sources* **2009**, *189*, 752.

(12) Hassoun, J.; Derrien, G.; Panero, S.; Scrosati, B. *Adv. Mater.* **2008**, *20*, 3169.

(13) Bridel, J. S.; Grugeon, S.; Laruelle, S.; Hassoun, J.; Reale, P.; Scrosati, B.; Tarascon, J.-M. *J. Power Sources* **2010**, *195*, 2036–2043.

(14) Arrebola, J. C.; Caballero, A.; Hernán, L.; Morales, J. *Electrochem. Solid-State Lett.* **2005**, *152* (3), 641–645.

(15) Caballero, A.; Cruz, M.; Hernán, L.; Melero, M.; Morales, J.; Rodriguez Castillón, E. *J. Electrochem. Soc.* **2005**, *152*, A552–A559.

(16) Thompson, A. H. *J. Electrochem. Soc.* **1979**, *126*, 608–16.

(17) Colin, J.-F.; Pralong, V.; Caignaert, V.; Hervieu, M.; Caveau, B. *Inorg. Chem.* **2006**, *45*, 7217–7223.

(18) Wen, C. J.; Boukamp, B. A.; Huggins, R. A.; Weppner, W. J. *Electrochem. Soc.* **1979**, *126*, 2258–66.

(19) Caballero, A.; Hernán, L.; Morales, J.; Angulo, M. *Electrochem. Solid-State Lett.* **2005**, *152* (1), 6–12.

NOTE ADDED AFTER ASAP PUBLICATION

In the version of this article published ASAP February 3, 2011, the last term in eq 2 was incomplete. The corrected version was published February 10, 2011.